

FOAM EMISSIVITY MODELS FOR MICROWAVE OBSERVATIONS OF OCEANS FROM SPACE

Magdalena D. Anguelova, Peter W. Gaiser, and Victor Raizer¹

Remote Sensing Division, Naval Research Laboratory, 20375, Washington DC, USA
Telephone: 202-404-6342; e-mail: magda@nrl.navy.mil

¹Zel Technologies, LLC, Fairfax, VA 22032, USA
Telephone: 703 764 2308; e-mail: vraizer@aol.com

ABSTRACT

Adequate accounting for the effect of the sea foam in forward models has the potential to improve the accuracy of satellite-based geophysical retrievals of environmental variables from passive radiometric measurements at frequencies from 1 to 100 GHz. Sea foam has a specific mechanical structure which gradually changes within the foam depth. Due to this vertical stratification, the foam characteristics acquire a wide range of values. To model the foam vertical stratification, it is necessary to use a vertical profile for the foam void fraction and to consider scattering between densely packed bubbles. In this study we evaluate two models which address the specifics of a vertically structured foam layer comprising densely packed bubbles in different ways.

Index Terms— Sea foam, foam fraction, microwave radiometer, WindSat, whitecaps.

1. INTRODUCTION

Increasing demands for accuracy in satellite-based geophysical retrievals of environmental variables from passive radiometric measurements at frequencies from 1 to 37 GHz necessitates forward geophysical models capable of adequate accounting for the foam effect [1], [2]. In addition, the direct and indirect involvement of whitecaps in numerous air-sea interaction and climate processes justifies work on parameterizing the high variability of whitecap coverage [3]. As a result there is a rekindled interest in measuring [4] and modeling [5] the microwave emissivity of sea foam, e_f .

For oceanographers, sea foam is defined broadly to include bubble plumes in the water, foam layers at the surface, and sea spray above. For remote sensing, the skin depth at microwave frequencies narrows the detection of the sea foam to its surface expression. Surface-layer foam has a specific mechanical structure [6] comprising densely packed

bubbles whose dimensions gradually change within the layer depth, Figure 1. Large, thin-walled bubbles in the upper part of the foam layer contain little seawater (dry foam). In depth, as bubbles become smaller and thick-walled, air content decreases (wet foam). Consequence of this vertical stratification of the foam structure is that all foam characteristics acquire a wide range of values. One thus needs a vertical profile to model the mechanical and dielectric properties of the sea foam, such as of the foam void fraction (f_a , defined as the fraction of a unit volume of seawater that is occupied by air) and foam complex dielectric constant (or permittivity, ϵ_f). To address the close packing of bubbles within the foam layer, scattering and dipole interaction between them should be considered. The question is how to achieve these two formidable tasks yet keep the model computationally efficient. In this study we evaluate two models which address the specifics of a vertically structured foam layer comprising densely packed bubbles in different ways.

2. EMISSIVITY MODELS

The macroscopic foam-spray model [7] (hereafter R07) represents the sea foam as a multilayer dielectric structure including layers of mono-dispersed bubbles, poly-dispersed bubbles, polyhedral bubbles, and sea spray. For this study the spray layer is “switched off.” The functional form for the void fraction profile, $f_a(z)$, is hyperbolic tangent. For regions of dry and wet foam, the profile of the effective foam permittivity in the layer depth, $\epsilon_f(z)$, is calculated with the Odelevskiy formula (hereafter Odel) and the modified Lorentz-Lorenz formula (hereafter L-L), respectively. Using the L-L formula, model R07 accounts for scattering within the foam layer. Model R07 applies an iterative numerical method to obtain the foam emissivity e_f with consecutive calculations of the complex Fresnel reflection coefficients.

The foam emissivity model [8], [6] (hereafter A06), uses an exponential void fraction profile to represent the vertical stratification of the sea foam. Following the conclusion that scattering in foam is weak [6], model A06 ignores scattering and calculates $\epsilon_f(z)$ with the Refractive mixing rule. A06 is a radiative transfer model (RTM), which obtains e_f by solving the radiative transfer equation with the so-called incoherent approach applicable for weakly scattering medium.

Models R07 and A06 are similar in that they both account for the stratification of foam void fraction $f_a(z)$ and the foam dielectric properties $\epsilon_f(z)$. The two models differ in three elements, namely (i) the functional form of $f_a(z)$; (ii) the mixing rule used for $\epsilon_f(z)$, which in fact represents inclusion/omission of scattering in foam; and (iii) the model chosen to compute the foam emissivity e_f .

Here we evaluate the differences between R07 and A06 in predicting ϵ_f , e_f , and brightness temperature due to foam, T_{BF} as affected by these different elements. All calculations are for 1 GHz to 100 GHz, H and V polarizations, seawater temperature of 10 °C, salinity of 34 psu, incidence angle of 53° and foam thicknesses $h = 1, 2, 3, 4, 5$, and 10 cm. The scattering in R07 is computed for mono-dispersed bubbles with radius $a = 0.05$ cm and ratio to bubble wall thickness of 0.01, which provides $f_a = 0.639$ for wet sub-layer of $h/10$ thickness. The seawater permittivity is computed with [9].

3. FOAM PERMITTIVITY COMPARISONS

Figure 2 shows the real parts of ϵ_f as predicted by the mixing rules with and without scattering. Panel (a) depicts the contributions to the foam permittivity from Odel and L-L formulae used in model R07. We see that the Odel formula (green lines in the graphs) is too low at high void fractions. When the scattering from poly-dispersed bubbles (red lines) is combined with it, the permittivity values of dry foam increase substantially. Meanwhile, scattering in mono-dispersed bubbles (blue lines) would only slightly change the Odel permittivity values for wet foam.

Panel (b) compares Odel formula (green lines again) with the Refractive mixing rule (black lines) used in model A06. The permittivity values for wet foam are very similar from both formulae, but for dry foam, the Refractive law predicts higher values. That is, the use of the Refractive law could compensate for ignoring scattering in A06.

4. FOAM EMISSIVITY COMPARISONS

We compare predictions of e_f with models R07 and A06 in 4 cases each time with one model element changed or added. Table 1 summarizes the input elements included for each case of model comparison.

In Case #1 both models use the same, linear profile for the void fraction and calculate foam permittivity with Odel formula, that is, scattering is not included in this case. The

only difference between the models is how e_f is computed, with Fresnel reflections or with RTM. This case, therefore, quantify the difference between R07 and A06 due to the model choice for computing e_f . In case #2 all elements in model A06 are the same, while in R07 we change only the computation of ϵ_f to include scattering with L-L formula. In this way we quantify the effect of including scattering on foam emissivity e_f . In case #3 all elements are as in case #2 only the computation of foam permittivity in model A06 is changed from Odel formula to Refractive law. This case, therefore, verifies the conclusion in [6] that the Refractive law is more suitable than other mixing rules for computing ϵ_f when scattering is ignored. Finally, case #4 quantifies differences between the two models due to use of different functional forms for the void fraction profile, hyperbolic tangent versus exponential. In each case we compare the models results in terms of percent difference (PD) defined as $\Delta X (\%) = 100 \cdot (X_{A06} - X_{R07}) / [(X_{A06} + X_{R07}) / 2]$.

Table 1

Case #	Model	$f_a(z)$	ϵ_f rule	L-L scatt	e_f model
1	R07	lin	Odel	No	Fresnel
	A06	lin	Odel	No	RTM
2	R07	lin	Odel	Yes	Fresnel
	A06	lin	Odel	No	RTM
3	R07	lin	Odel	Yes	Fresnel
	A06	lin	Refr	No	RTM
4	R07	tanh	Odel	Yes	Fresnel
	A06	exp	Refr	No	RTM

The comparisons show the following: The main differences between models R07 and A06 are due to the choice of the model computing e_f . (Case #1). PDs could be above 20% up to 100% for thin foam layers (1 cm) and lower frequencies (below 5 GHz), H polarization. In most cases, however—frequencies above 5 GHz, V pol and thick foam (above 1 cm)—the models differ by no more than 20%. When scattering is included (Case #2), PDs between the models change (increase or decrease) by no more than 20% (black lines in Figure 3c). That is, the choice of e_f model is more consequential than including or ignoring scattering. The lowest differences between models are for Case #3 (Figure 3a and red lines in 3c). We interpret this as confirmation that using the Refractive law to obtain foam permittivity compensates to some degree the ignoring of scattering. Case #4 (Figure 3b and blue lines in 3c) shows that the models are quite sensitivity to the functional form of the void fraction.

5. BRIGHTNESS TEMPERATURE DUE TO FOAM

A foam emissivity model predicts the emissivity of an area fully covered with foam. To put these modeled values of foam emissivity into practical use, we show here how they

can be used to obtain the brightness temperature due to foam, T_{Bf} , for ocean conditions. In addition we compare these modeled T_{Bf} with first estimates of T_{Bf} from satellite-based data.

The procedure of obtaining and mapping the ‘modeled’ T_{Bf} is shown with the red blocks in Figure 4a. We calculate e_f with a foam emissivity model (e.g., R07 or A06) and combine these e_f values with the physical seawater temperature T_s and the foam fraction W to obtain ‘modeled’ T_{Bf} in the ocean. The foam fraction W can be obtained using wind speed U_{10} with one of the various parameterizations available in the literature. In this study we use the parameterization [10] for neutral atmosphere. We also used other formulae for W and concluded that the main uncertainty in obtaining ‘modeled’ T_{Bf} comes from the choice of $W(U_{10})$ parameterization. This is noted in Figure 4a with red shading of the block for W . T_s and U_{10} can be obtained from satellites (e.g., QuikSCAT) or from weather prediction models (e.g., GDAS at NCEP, Global Data Assimilation System at National Centers for Environmental Prediction). The ‘modeled’ T_{Bf} is mapped on the globe using the (lat,lon) locations of U_{10} and T_s .

The green blocks in Figure 4a visualize our procedure of obtaining the ‘measured’ T_{Bf} . For this we use WindSat measurements of T_B at the top of the atmosphere (TOA) matched in time and space with U_{10} and T_s from QuikSCAT and GDAS. We also use the WindSat forward model to obtain T_B due to rough surface with the 2-scale model. The 2-scale model is tuned for roughness only [1] and does not include the effect of foam. It is run with the U_{10} and T_s match-ups. Match-ups with data from SSM/I (Special Sensor Microwave/Imager) are used to make atmospheric correction of the TOA T_B from WindSat and from the 2-scale model and obtain T_B at the ocean surface. Taking the difference between these two surface estimates, $T_B(\text{WS})$ and $T_B(2s)$, we obtain the ‘measured’ T_{Bf} . The differencing $T_B(\text{WS}) - T_B(2s)$ minimizes the uncertainty due to atmospheric correction and match-ups. Error analysis shows that error due to inaccuracies in U_{10} and T_s are small, at most 1%. The main uncertainty in estimating measured T_{Bf} comes from modeling errors in the 2-scale model (noted in Figure 4a with green shading of the ‘2-scale’ block), which are difficult to quantify.

The ‘measured’ T_{Bf} for the Southern Ocean (August 2006) are mapped (Figure 4b) and compared with the corresponding maps of ‘modeled’ T_{Bf} (Figures 4c-d). Figures 4e-f show difference maps (model minus WindSat) corresponding to the models predictions in Figures 4c-d.

6. SUMMARY

In this paper, we report new developments in modeling the sea foam emissivity useful for space-based microwave observations of the ocean surface. Two foam emissivity models at microwave frequencies are considered and

compared in details. Bubble’s properties are the main microstructure factor. Effective permittivity and emissivity values are computed for a wide range of frequencies from 1 to 100 GHz. Effects of scattering and dielectric stratifications (profiles) are evaluated numerically. Scattering and profiles contributions affect models prediction most in frequency range from 1 to 40 GHz. Both models are suitable for ocean studies from space. So-called “Foam coverage signatures” are generated from WindSat and model data for the first time.

7. REFERENCES

- [1] M.H. Bettenhausen, C.K. Smith, R.M. Bevilacqua, N.-Y. Wang, P.W. Gaiser, and S. Cox, “A nonlinear optimization algorithm for WindSat wind vector retrievals,” *IEEE Trans. Geosci. Rem. Sens.*, 44, pp. 597-610, Mar. 2006.
- [2] A. Camps, et al., “Determination of the sea surface emissivity at L-band and application to SMOS salinity retrieval algorithms: Review of the contributions of the UPC-ICM,” *Radio Sci.*, 43, RS3008, doi:10.1029/2007RS003728, 2008.
- [3] M.D. Anguelova and F. Webster, “Whitecap coverage from satellite measurements: A first step toward modeling the variability of oceanic whitecaps,” *J. Geophys. Res.*, 111, C03017, doi:10.1029/2005JC003158, Mar. 2006.
- [4] L.A. Rose, W.E. Asher, S.C. Reising, P.W. Gaiser, K.M. St Germain, D.J. Dowgiallo, K.A. Horgan, G. Farquharson, and E.J. Knapp, “Radiometric measurements of the microwave emissivity of foam,” *IEEE Trans. Geosci. Remote Sens.*, 40, pp. 2619–2625, Dec. 2002.
- [5] D. Chen, L. Tsang, L. Zhou, S.C. Reising, W.E. Asher, L.A. Rose, K.-H. Ding; C.-Te Chen, “Microwave emission and scattering of foam based on Monte Carlo simulations of dense media,” *IEEE Trans. Geosci. Rem. Sens.*, 41, pp. 782 – 790, Apr. 2003.
- [6] M.D. Anguelova, “Complex dielectric constant of sea foam at microwave frequencies,” *J. Geophys. Res.*, 113, C08001, doi:10.1029/2007JC004212, Aug 2008.
- [7] V. Raizer, “Macroscopic Foam–Spray Models for Ocean Microwave Radiometry,” *IEEE Trans. Geosci. Rem. Sens.*, vol.45, no.10, pp.3138-3144, Oct. 2007.
- [8] M.D. Anguelova, M.H. Bettenhausen, and P.W. Gaiser, “Passive remote sensing of sea foam using physically-based modes,” *IEEE Proceed. Geosci. Rem. Sens Symp. (IGARSS’06)*, 7, pp. 3676–3679, 2006.
- [9] A.P. Stogryn, “Equations for the permittivity of sea water,” *Report to NRL Washington DC*, 11 pp., GenCorp Aerojet, Azusa, CA, 1997.
- [10] E. Monahan and I. O’Muircheartaigh, “Whitecaps and the passive remote sensing of the ocean surface,” *Int. J. Remote Sens.*, 7, pp. 627–642, 1986.

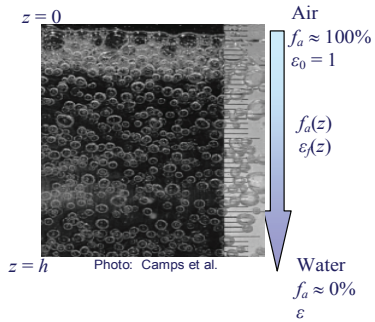


Figure 1 Vertically stratified foam layer.

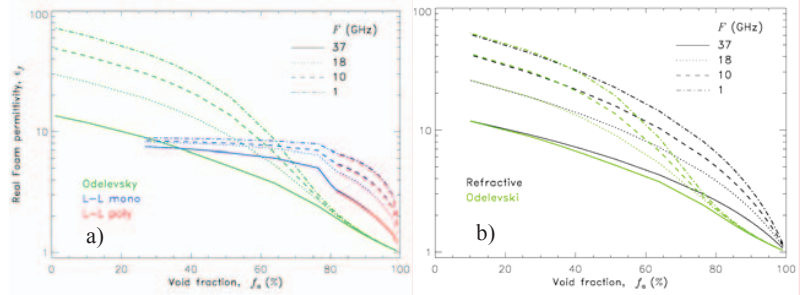


Figure 2 Real part of foam permittivity: a) Scattering contribution; b) No scattering.

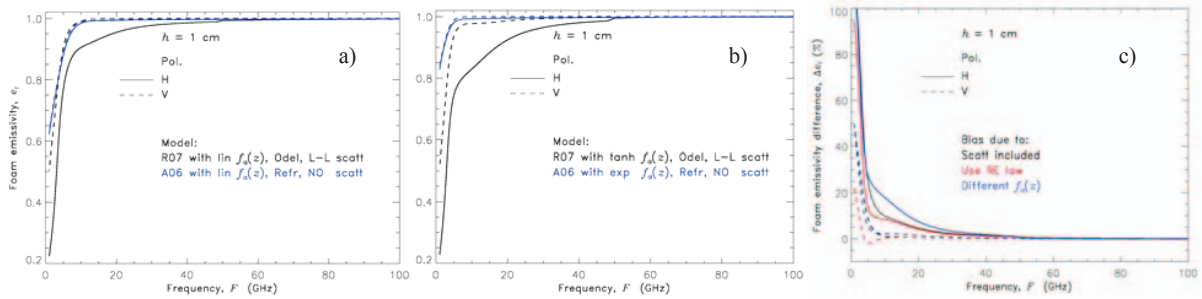


Figure 3 Comparison of models predictions of foam emissivity: a) Scattering vs No scattering; b) With different void profiles; c) Model differences quantified in terms of percent difference for different cases (see Table 1).

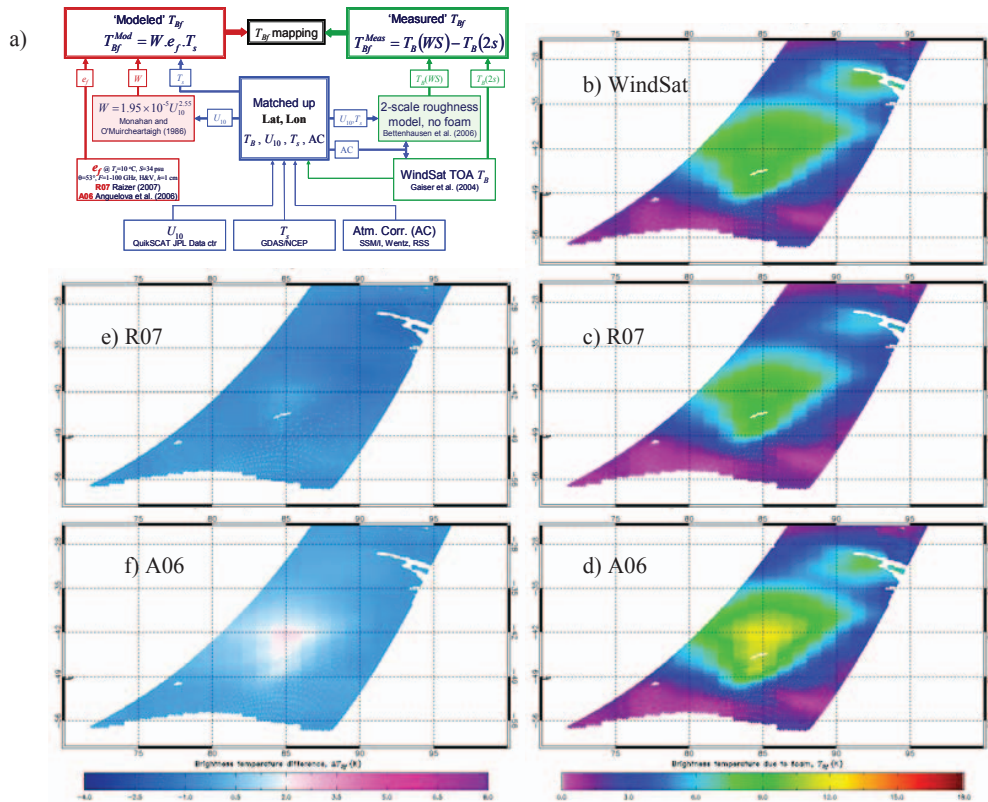


Figure 1 Foam coverage signature, T_{Bf} , in Southern ocean, August 2006: a) Flow-chart of procedures of computation; b) Measured T_{Bf} from WindSat data; c) Modeled T_{Bf} with R07; d) Modeled T_{Bf} with A06; e-f) Difference maps (model minus WindSat) respective to panels c and d.